

Neurons in the lateral part of the lumbar spinal cord show distinct novel axon trajectories and are excited by short propriospinal ascending inputs

Zs. Antal¹ · L. L. Luz² · B. V. Safronov² · M. Antal^{1,3} · Peter Szücs^{2,4,5} 

Received: 30 December 2014 / Accepted: 15 April 2015 / Published online: 26 April 2015
© Springer-Verlag Berlin Heidelberg 2015

Abstract The role of spinal dorsal horn propriospinal connections in nociceptive processing is not yet established. Recently described, rostrocaudally oriented axon collaterals of lamina I projection and local-circuit neurons (PNs and LCNs) running in the dorsolateral funiculus (DLF) may serve as the anatomical substrate for intersegmental processing. Putative targets of these axons include lateral dendrites of superficial dorsal horn neurons, including PNs, and also neurons in the lateral spinal nucleus (LSN) that are thought to be important integrator units receiving, among others, visceral sensory information. Here we used an intact spinal cord preparation to study intersegmental connections within the lateral part of the superficial dorsal horn. We detected brief monosynaptic and prolonged polysynaptic excitation of lamina I and LSN neurons when stimulating individual dorsal horn neurons located caudally, even in neighboring spinal cord segments. These connections, however, were infrequent. We also revealed that some projection neurons outside the

dorsal grey matter and in the LSN have distinct, previously undescribed course of their projection axon. Our findings indicate that axon collaterals of lamina I PNs and LCNs in the DLF rarely form functional connections with other lamina I and LSN neurons and that the majority of their targets are on other elements of the dorsal horn. The unique axon trajectories of neurons in the dorsolateral aspect of the spinal cord, including the LSN do not fit our present understanding of midline axon guidance and suggest that their function and development differ from the neurons inside lamina I. These findings emphasize the importance of understanding the connectivity matrix of the superficial dorsal horn in order to decipher spinal sensory information processing.

Keywords Lateral spinal nucleus · Propriospinal connection · Midline crossing · Ipsilateral projection · Bilateral projection · 3-D reconstruction

✉ Peter Szücs
szucs.peter@med.unideb.hu

¹ Department of Anatomy, Histology and Embryology, University of Debrecen, Nagyerdei krt. 98, Debrecen 4032, Hungary

² Neuronal Networks Group, Instituto de Biologia Molecular e Celular-IBMC, Universidade do Porto, Rua do Campo Alegre 823, 4150-180 Porto, Portugal

³ MTA-DE Neuroscience Research Group, Debrecen 4012, Hungary

⁴ MTA-DE-NAP B-Pain Control Research Group, Nagyerdei krt. 98, Debrecen 4032, Hungary

⁵ Department of Physiology, University of Debrecen, Nagyerdei krt. 98, Debrecen 4032, Hungary

Introduction

It is generally accepted that the nociceptive information conveyed by primary afferent fibers is processed, modulated and integrated by neuronal networks of the superficial dorsal horn before being transmitted to supraspinal centers by projection neurons (PNs; Todd 2010). Our knowledge about the architecture and exact function of these networks, which is crucially needed for identifying new analgetic targets, is yet far from being complete.

While propriospinal connections are of major importance in coordinating locomotor actions (Etlin et al. 2010; Juvin et al. 2005), most attempts to map dorsal horn connectivity focused on segmental neuronal circuits mainly

due to limitations of the spinal cord slice technique. Based on paired electrophysiological recordings, Lu and Perl (2003, 2005) suggested that the superficial dorsal horn is organized into neuronal modules, in which specific neuron types establish highly selective connections with each other. According to their observations, central cells of the inner part of lamina II establish monosynaptic excitatory connections with vertical neurons of the outer lamina II. These in turn excite lamina I projection and non-projection cells, providing a ventral to dorsal excitatory drive to lamina I (Braz et al. 2014). This model is in line with the results of Santos et al. (2007), who emphasize that sensory processing in the dorsal horn is dominated by excitatory connections, and those of Kato et al. (2009), who report that the translaminal input pattern is greater in case of lamina I neurons and vertical cells than in cases of other neurons in the superficial dorsal horn.

These translaminal network models do not take into account connections from neighboring or distal segments of the spinal cord. Interestingly, almost half a century ago Szentagothai (1964) already reported that lamina II neurons establish short-range propriospinal connections via an intrinsic longitudinal unmyelinated axon system, which bridges distances of 2–3 mm. Functional evidence for such connections has been later provided by laser-scanning photostimulation experiments (Kato et al. 2009). Besides the short-range connections, Szentagothai (1964) also proposed a long-range propriospinal connection system via the lateral part of Lissauer's tract, which can bridge 5–6 spinal segments. Indeed, widespread propriospinal connectivity was confirmed by exhaustive axon-tracing experiments in the medial and lateral aspect of the dorsal horn (Petko and Antal 2000; Petko et al. 2004).

Although the composition of the intrinsic longitudinal unmyelinated axon system in the lateral aspect of the superficial dorsal horn is not fully described it undoubtedly contains ipsilateral collaterals of PNs in lamina I (Szucs et al. 2010) and a large number of thin axons that belong to lamina I local-circuit neurons (LCNs; Szucs et al. 2013). Potential targets of such axon collaterals include lateral dendrites and soma of lamina I cells and neurons scattered among the fibers of the dorsolateral funiculus (DLF), forming a continuous column ventrolateral to the dorsal horn of the spinal cord, termed lateral spinal nucleus (LSN) by Gwyn and Waldron (1968, 1969) who first described the structure. LSN neurons can be activated by noxious stimulation (Olave and Maxwell 2004), receiving afferent input from C-fibers innervating muscles (Olave and Maxwell 2004) and viscera (Sugiura et al. 1989) and project through ascending tracts to the brainstem, hypothalamus, and thalamus (Menetrey et al. 1982; Pechura and Liu 1986; Menetrey and Basbaum 1987; Leah et al. 1988; Burstein

et al. 1990). At the same time little is known about the input to LSN cells from neighboring neurons and almost nothing about the course and local branching of their axon. Presence of considerable amount of peptidergic varicosities is characteristic of the nucleus (Olave and Maxwell 2004) and the number of peptidergic varicosities is not affected by dorsal rhizotomy or experimental lesions of the descending pathways, therefore several authors conclude that peptidergic input to LSN may arise from the same or nearby segmental levels of the spinal cord. (Seybold and Elde 1980; Cliffer et al. 1988; Giesler and Elde 1985; Olave and Maxwell 2004).

Our hypothesis was that lateral collaterals of PNs and the extensive unmyelinated axon of lamina I LCNs may contribute to functional short propriospinal connections to rostral lamina I and LSN neurons (Fig. 1a). By using an *in vitro* intact lumbar spinal cord preparation and oblique IR-LED illumination (Szucs et al. 2009), we showed that cell-attached stimulation of lamina I neurons evoked both mono- and polysynaptic excitation in neurons of lamina I and the LSN in the neighboring rostral segments. However, the low frequency of such connections suggests that major targets of this propriospinal axon system are not lamina I and LSN neurons. At the same time, 3-D reconstruction of the postsynaptic neurons revealed novel axon trajectories of LSN and lateral lamina I neurons.

Materials and methods

Spinal cord preparation

Laboratory Wistar rats (P14–P24) were killed in accordance with the European Community Council Directives and national guidelines (Direcção Geral de Veterinária, Ministério da Agricultura and the Animal Care and Protection Committee at the University of Debrecen) after anesthesia with intraperitoneal injection of Na⁺-pento-barbital (30 mg/kg) and subsequent check for lack of pedal withdrawal reflexes. The vertebral column was quickly cut out and immersed in oxygenated artificial cerebrospinal fluid (ACSF) at room temperature. The lumbar spinal cord was dissected, dorsal and ventral roots were carefully cut and the pia mater was locally removed in the region of interest for the recording and stimulating pipettes. The spinal cord was glued with cyanoacrylate adhesive to a golden plate with the dorsolateral spinal cord surface facing upwards, and transferred to the recording chamber. In some cases more than one cell was recorded in the same spinal cord preparation. The total number of animals used in this study was 73. All recordings were performed at 22–24 °C.

Selection of neurons and visual field counting

Lamina I and LSN neurons were visualized in the intact lumbar spinal cord using the oblique IR-LED illumination technique (Safronov et al. 2007; Szucs et al. 2009). Postsynaptic neurons with large somata (above 20 μ measured on the screen) were selected in the superficial layer of the lateral edge of the dorsal grey matter and in the adjacent DLF. Prior to the morphological confirmation neurons were considered to be located in the LSN if they were scattered between fibers of the DLF (see Fig. 1 in Pinto et al. 2010). After establishing whole-cell configuration with the postsynaptic neuron 2–3 landmark structures were noted at the caudal end of the view-field. Then, the objective of the microscope was moved caudally along the spinal cord until the landmarks disappeared at the rostral end of the view-field and putative presynaptic neurons were searched for in this region. The size of a single visual field under our conditions was approximately 180 μ m (see Fig. 9b in Szucs et al. 2009). When measuring larger rostrocaudal distances from the postsynaptic neuron, the above steps were performed repeatedly. A schematic representation of the view-fields along the rostrocaudal extent of the preparation along with the position of the postsynaptic neuron is shown in Fig. 1b.

Whole-cell patch-clamp recording, cell-attached stimulation and neuron filling

Recordings from lamina I neurons were made in whole-cell mode. The ACSF contained (in mM): NaCl 115, KCl 3, CaCl₂ 2, MgCl₂ 1, NaH₂PO₄ 1, NaHCO₃ 25, and glucose 11 (pH 7.4 when bubbled with 95–5 % mixture of O₂–CO₂). Pipettes were pulled from thick-walled glass (Bio-Medical Instruments, Germany) and fire-polished (resistance, 3–5 M Ω). The pipette solution contained (in mM): KCl 3, K-gluconate 150, MgCl₂ 1, BAPTA 1, HEPES 10 (pH 7.3 adjusted with KOH, final [K⁺] was 160 mM) and 0.5–1 % biocytin to allow consecutive morphological identification of the neurons. The majority of the recordings were made with an EPC10-Double amplifier (HEKA, Lambrecht, Germany). The signal was low-pass filtered at 2.9 kHz and sampled at 10 kHz. Offset potentials were compensated before seal formation. Liquid junction potentials were calculated (15.9 mV) and corrected for in all experiments using the compensation circuitry of the amplifier. Intact presynaptic neurons were selectively stimulated through a cell-attached pipette (Santos et al. 2007) containing 500 mM NaCl and 1.5 % biocytin. Pairs of monosynaptically connected neurons were identified by using a protocol that contained a pre-pulse period (200 ms) followed by a single current pulse (100 nA, 1 ms) and a

post-pulse recording period (200 ms) in which the postsynaptic neuron was recorded for 200 ms preceding and 200 ms following a current pulse application (100 nA, 1 ms) to the presynaptic neuron, and by analyzing the stimulus-evoked changes in the excitatory postsynaptic current (EPSC) numbers. In some cases the pre-pulse recording was shorter (20 ms). The protocol was repeated 90 times at 1 Hz. EPSC latencies in connections were calculated from the end of the 1 ms stimulation pulse to the time moment when the evoked EPSC reached 10 % of its peak amplitude. EPSCs in the pre- and post-pulse period were detected automatically by using MiniAnalysis (Synaptosoft, 3098 Anderson Place, Decatur, GA 30033, USA). Postsynaptic responses were considered monosynaptic if evoked EPSCs showed a low failure rate and a latency variation below 4 ms. These criteria were based on our prior study in the intact spinal cord preparation (Luz et al. 2010) showing that lamina I neurons are directly connected by several parallel synapses via axodendritic pathways of different length, and therefore, latencies of individual components of a monosynaptic EPSC recorded in one connection can differ substantially. The monosynaptic nature of the connection was also verified by confirming the presence of transitions between individual EPSC components (see Santos et al. 2009; Luz et al. 2010). Some recordings were done with an Axopatch 1D amplifier (Molecular Devices, LLC, 1311 Orleans Drive Sunnyvale, CA 94089 USA). In these cases cell-attached stimulation of putative presynaptic neurons were carried out with an Axoclamp 2B amplifier (Molecular Devices, LLC, 1311 Orleans Drive Sunnyvale, CA 94089 USA).

Visualization of filled neurons

After fixation in 4 % formaldehyde, the spinal cord was embedded in agar and 100- μ m-thick sagittal serial sections were prepared with a tissue slicer (Leica VT 1000 S). To reveal biocytin, sections were permeabilized with 50 % ethanol and treated according to the avidin-biotinylated horseradish peroxidase (HRP) method (ExtrAvidin-Peroxidase, diluted 1:1000; Sigma, St. Louis, MO) followed by a diaminobenzidine (DAB) chromogen reaction. Sections were either counterstained on slides with 1 % toluidine blue, dehydrated, cleared and coverslipped with DPX (Fluka, Buchs, Switzerland), or treated with 1 % OsO₄ and embedded in epoxy resin (Durcupan, Fluka, Buchs, Switzerland). Photomicrographs were taken using the 10 \times or 40 \times dry lens of a Primo Star (Zeiss) microscope equipped with a Guppy (Allied Vision Technologies) digital camera. Contrast and brightness of the photographic images used in all the figures were adjusted using the Adobe Photoshop software.

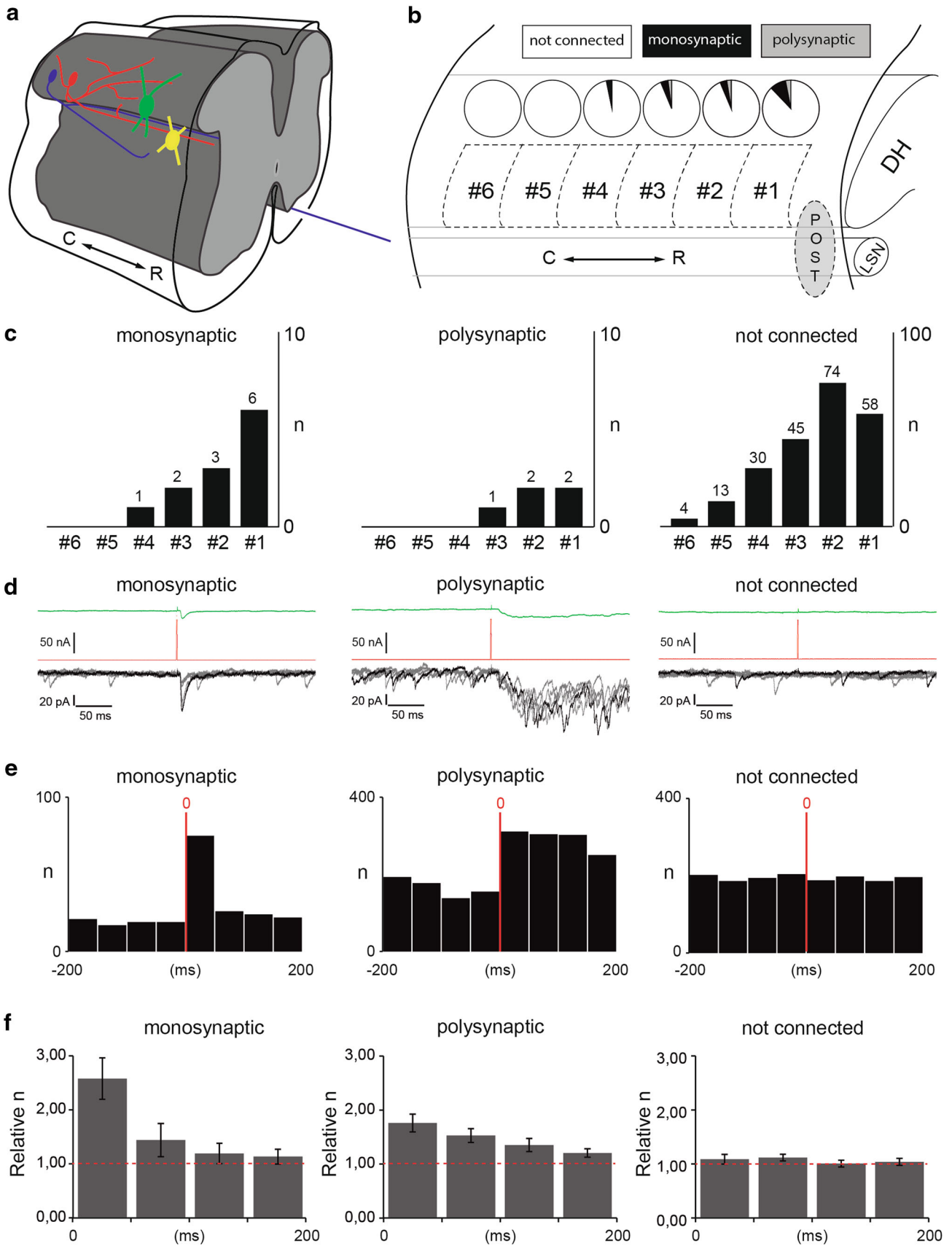


Fig. 1 Short mono- and polysynaptic propriospinal connections of lateral lamina I and LSN neurons. **a** Hypothetic wiring of short propriospinal connections via unmyelinated axons. Lateral axon collaterals of projection neurons (PNs; *blue cell*) and rostrocaudal axons of local-circuit neurons (LCNs; *red neuron*) may contact lateral lamina I neuron (*green cell*) dendrites and LSN neurons (*yellow cell*) in the dorsolateral funiculus (DLF). **b** Schematic illustration of the recording regions on the preparation. The *grey ellipse* represents the region where the postsynaptic neuron was located. *Squares* shown by *dashed lines* indicate the different view-fields. The *incrementing numbers* refer to the distance from the postsynaptic region. Pie chart above each view-field shows the percentage of neurons with monosynaptic (*black*) and polysynaptic connection with the postsynaptic neurons. (DH, dorsal horn; LSN, lateral spinal nucleus; POST, postsynaptic neuron; C, caudal; R, rostral). **c** Number of neurons per view-field that had monosynaptic (*left*), polysynaptic (*middle*) or no connection (*right*) onto the postsynaptic neurons. **d** Representative voltage-clamp traces of a monosynaptic connection (*left*), a polysynaptic connection (*middle*) and a case where the stimulated neuron was not connected to the recorded one (*right*). In *each panel* the *green trace* on the *top* shows the averaged postsynaptic current, the *red trace* below shows the cell attached stimulation protocol of the presynaptic neuron (200 ms long recordings before and after the 1-ms current step injection into the presynaptic neuron). *Bottom traces* show five non-consecutive individual voltage traces recorded in the postsynaptic neuron (for clarity one is highlighted in *black*). **e** Cumulative number of excitatory postsynaptic currents (EPSCs) from 90 consecutive traces in 50-ms bins before and after the transient stimulation of the presynaptic neuron in case of a monosynaptic pair (*left*), a polysynaptic connection (*middle*) and in a case where the stimulated neuron did not evoke a response in the postsynaptic one (*right*). *Red vertical lines* indicate the time point (0 ms), when the presynaptic neuron was stimulated. Note the differences on the *Y axis*. **f** Normalized cumulative EPSC numbers from 90 consecutive trials in 50-ms bins following stimulation in monosynaptic pairs (*left*, $n = 8$), polysynaptic connections (*middle*, $n = 5$) and cases where the neurons were not connected (*right*, $n = 5$). The *red dashed line* indicates the average number of EPSCs recorded during the 200-ms period preceding stimulation

3-D reconstruction and analysis

Complete 3-D reconstructions were performed from serial sagittal sections with NeuroLucida (MBF Bioscience, 185 Allen Brook Lane, Suite 101 Williston, VT 05495 USA). First, each section was completely traced into the corresponding section of a serial section dataset with a 40× (dry) objective. Caliber of the digitally traced processes was continuously matched with the video image of the labeled process. Fiber caliber units for the selected lens were automatically set by the software, based on prior calibration. Whenever necessary, a 100× (oil immersion) lens was used to determine the Z difference between crossing structures. Next, we aligned the sections and connected the pieces working always towards the section containing the soma. Due to shrinkage the thickness (Z dimension) of resin-embedded sections was 80–90 % of the original 100 μm. This was comparable with shrinkage of these long sagittal spinal cord sections along the X–Y

axes. Thus, Z-shrinkage was not corrected in these cases. In the case of DPX-embedded material the shrinkage along the Z-axis was corrected to reach a thickness of 80 μm. In most cases, tracing and the procedure of alignment followed by connecting the corresponding pieces were performed by independent persons, to ensure a double check for all reconstructions. Section contours as well as gray matter and central canal borders were traced at the bottom level of each section. In Figs. 4, 5 and 6 the 3-D reconstructions of neurons are shown in schematic spinal cord outlines that were adjusted to the actual contours of the given reconstruction. Special care was taken that the position of the central canal and the borders of the grey and white matter fall as close as possible to the real contours. Graphical rendering of the 3-D structures was performed by Py3DN (Aguiar et al. 2013; <https://sourceforge.net/projects/py3dn/>) in Blender, a well-established free open source 3-D content creation suite (<http://www.blender.org>). All 3-D reconstructions will be submitted to <http://NeuroMorpho.Org>.

Morphometric analyses and basic quantitative measurements including Sholl analysis, dendritic segment length calculation, spine numbers, spine density and Fan-In projection were performed by NeuroLucida Explorer (MBF Bioscience, 185 Allen Brook Lane, Suite 101 Williston, VT 05495 USA). During the Fan-in projection a vertical axis is placed through the neuron. A virtual plane is swept around the axis collecting tracings of the dendritic structures. After sweeping through a full 360° the plane has collected all of the dendritic structures that appear on the same side of the plane. The fan-in projection was used to understand any preferred orientation in the dendritic processes. The fan in grid displays distance and angle. The processes are aligned so that all begin at the origin of the grid. Randomly oriented processes evenly cover the grid. Preferentially oriented processes trend more in some directions than other directions.

Statistical analysis

All statistical analyses were performed with the SigmaStat 3.0 (Systat Software, San Jose, CA, USA) software. Comparison of morphometric parameters between lamina I neurons and cells in the lateral adjacent white matter and LSN was done by using Student's *t* test or Mann–Whitney Rank Sum test. Between-group comparisons of EPSC kinetic parameters were done by Kruskal–Wallis one-way analysis of variance on ranks followed by Dunn's pairwise multiple comparison. A $p < 0.05$ was considered to be statistically significant.

Numbers are given as mean ± SEM unless otherwise mentioned.

Results

In this study, altogether 86 cells were recorded in whole cell mode in the lateral aspect of the spinal dorsal horn and in the LSN. Although post hoc visualization of biocytin in the recorded neuron was attempted in all cases, successful recovery, that allowed confirmation of the location and classification of the axon and somatodendritic domain, has only been achieved in 32 cases (recovery rate: 37 %; Table 1).

Electrophysiological properties and synaptic connectivity

Recorded cells had a mean resting membrane potential of -58.6 ± 1.6 mV ($n = 84$), while the mean input resistance and the membrane time constant were 435 ± 45 M Ω ($n = 84$) and 75.2 ± 10.4 ms ($n = 56$), respectively. For 54 whole-cell-recorded cells we tested 241 putative presynaptic neurons by cell-attached stimulation (the numbers of trials for a single postsynaptic neuron ranged from 1 to 18). Most presynaptic cells tested were selected in the three neighboring segments caudal to the location of the postsynaptic neuron (Fig. 1b, c). In 224 cases, stimulation of the presumably presynaptic cell did not evoke response in the postsynaptic neuron. These cells were evaluated as not connected (Fig. 1c–f). The lack of possible mono- or polysynaptic connection was also apparent from the unchanged frequency of excitatory postsynaptic currents (EPSCs) in the 200-ms-long periods before and after the 1-ms-long presynaptic stimulation (Fig. 1d–f). In 12 cases, stimulation of the presynaptic neuron resulted in a reliably evoked EPSC (Fig. 1d) with a mean latency of 5.7 ± 1.5 ms ($n = 12$, range of the means 1.7–19.8 ms) and mean latency variation of 2.9 ± 0.4 ms. The mean amplitude of the monosynaptic EPSCs was 30.7 ± 5.2 pA ($n = 12$, range of the means 6.6–63.4 pA). The stable response caused marked increase in the frequency of EPSCs within the first 50-ms period after the stimulation (Fig. 1e, f). The occurrence of monosynaptic connections was highest when looking for presynaptic neurons in the first visual field caudal to the postsynaptic recording site and decreased gradually when searching for presynaptic neurons more caudally. The most distant monosynaptically connected neuron was found four visual fields (720 μ m) away, from the postsynaptic neuron (Fig. 1c). This distance is comparable with the length of shorter lumbar segments in the juvenile rat spinal cord (Szucs et al. 2013). In case of five paired recordings stimulation of the presynaptic neuron initiated a huge increase of the basal EPSC frequency. Interestingly, this was sustained in the postsynaptic neuron for hundreds of

milliseconds without further stimulation of the presynaptic cell, possibly due to activation of polysynaptic excitatory pathways (Fig. 1d). For this reason we called this type of connection polysynaptic. A well-defined monosynaptic component in these connections could not be identified due to the complex kinetics of the summed EPSCs (Fig. 1d). When normalized to the EPSC frequency of the 200-ms-long pre-stimulus period the EPSC increment was highest in the first 50-ms-long bin and showed a gradual decrease unlike the abrupt difference after the first 50-ms period of the monosynaptic connections (Fig. 1f).

Efficacy of the polysynaptic input, electrophysiological properties and synaptic connectivity

Next, we wanted to see how effective the long-lasting EPSC frequency increase was in evoking action potentials in the five neurons receiving polysynaptic input. Thus, we repeated the same protocol (200 ms pre-stimulus and 200 ms post-stimulus periods) in current-clamp mode. The consecutive EPSPs were capable of depolarizing the neurons above the firing threshold even from membrane potentials as low as -90 mV (Fig. 2a). At around -80 mV stimulation of the presynaptic neuron resulted in sustained tonic action potential discharge (Fig. 2b). The frequency of the discharge evoked by this synaptic input stimulation was visibly lower than that evoked by a somatically injected current pulse causing depolarization of similar amplitude, about 10–15 mV (Fig. 2c). When normalized to the pre-stimulus period, the mean number of action potentials (for all the neurons with polysynaptic input, $n = 5$) showed a 5-fold increase in the post-stimulus epoch (Fig. 2d). From the five neurons with polysynaptic input, one (shown in Fig. 2) was an LCN in the most lateral part of lamina I with its dendrites protruding mostly into DLF and to a negligible extent into the dorsal horn. Two other cells were outside lamina I but not within the region of the LSN, while the remaining two cells were not filled sufficiently for morphological identification.

General somatodendritic features of neurons outside the dorsal grey matter

From the 32 neurons, in which biocytin was successfully recovered, only 5 cells were located within the boundaries of lamina I (cells 1–5; Table 1). The rest of the cells were next to the lateral edge of lamina I, among the superficial fibers of the DLF ($n = 18$; cells 6–23) or within the LSN ($n = 9$; cells 24–32). While neurons within lamina I could be classified according to the system introduced by Lima and Coimbra (1986), neurons located more laterally,

Table 1 Position, somatodendritic type and axon trajectory of the recovered neurons

cell No	position	soma / dendrite (Lima and Coimbra, 1986)	axon			3-D
			midline crossing	ascending	ipsilateral collaterals	
1	L-I	flattened	AC	c-ALT	DCT	
2	L-I	fusiform	AC	c-ALT	MCT	
3	L-I	flattened	AC	c-ALT	-	
4	L-I	flattened	AC	c-ALT	LCT	
5	L-I	Flattened	-	-	LCN	
6	OUT	NA	AC	c-ALT	-	
7	OUT	pyramidal	AC	c-ALT	MCT	
8	OUT	NA	PC-AC	i-ALT	L-III/IV, L-X	+
9	OUT	NA	PC	c-ALT	L-IV	+
10	OUT	multipolar	-	-	LCN	+
11	OUT	NA	AC	c-ALT	MCT	
12	OUT	NA	AC	c-ALT	DCT	
13	OUT	NA	AC	c-ALT	-	
14	OUT	flattened	AC	c-ALT	LCT	
15	OUT	NA	PC	c-ALT	-	
16	OUT	NA	AC	c-ALT, i- DLF	DLF-caudal, L-I, L-III/IV	+
17	OUT	NA	AC	c-ALT, i- DLF	Lissauer-tract	+
18	OUT	NA	-	-	LCN	
19	OUT	NA	PC-AC	i-ALT	L-III/IV	+
20	OUT	NA	PC-AC	i-ALT	L-III/IV, L-X, L-VII	+
21	OUT	NA	PC	c-ALT	L-I/II	+
22	OUT	NA	PC	c-ALT	L-III/IV*, L-X*	+
23	OUT	NA	AC	c-ALT	MCT	
24	LSN	NA	PC	c-ALT	DLF, L-X	+
25	LSN	NA	AC	c-ALT, i- DF	DLF-caudal	+
26	LSN	NA	AC	c-ALT, i- DF	DLF-caudal	+
27	LSN	NA	PC-AC	i-ALT	-	+
28	LSN	NA	PC	c-ALT	L-VII	+
29	LSN	NA	-	-	LCN	
30	LSN	NA	PC	c-ALT	L-V/VI, L-X	+
31	LSN	NA	AC	c-ALT	MCT	
32	LSN	NA	PC-AC	i-ALT	L-V/VI	+

Bold values indicate neurons with a projection axon crossing in the posterior commissure and ascending in the c-ALT. Italic values indicate double crossing i-ALT ascending neurons. Bold italic values indicate neurons with bilateral (ipsi and contra) ascending axon

L-I lamina I, *OUT* between the lateral edge of the dorsal grey and the LSN, *LSN* lateral spinal nucleus, *NA* not applicable, *AC* anterior commissure, *PC* posterior commissure, *c-ALT* contralateral anterolateral tract, *i-ALT* ipsilateral anterolateral tract, *DLF* dorsolateral funiculus, *DF* dorsal funiculus, *L-I-X* lamina I-X, *3-D* neuron reconstructed in three-dimensions with NeuroLucida, *DCT* dorsal collateral type projection neuron (see Szucs et al. 2010), *MCT* mixed collateral type projection neuron (see Szucs et al. 2010), *LCTT* lateral collateral type projection neuron (see Szucs et al. 2010)

outside the dorsal grey matter and in the LSN, with the exception of three cells (Table 1) presented very different somatodendritic features. We compared basic morphometric parameters of these neurons with a pooled sample of 3-D reconstructed PNs and LCNs ($n = 4$ for each, L-I in Fig. 3) from our earlier works (Luz et al. 2010; Szucs et al. 2013). Neurons lateral to lamina I and in the LSN had more stem dendrites (Fig. 3d) and significantly longer total

dendritic length (summed dendritic segment length; Fig. 3e; $p < 0.05$, Student's *t* test). This difference was apparent in the generally more “bushy” appearance of neurons outside lamina I (Fig. 3a, b). Another striking feature of the neurons lateral to lamina I was the presence of numerous short spines along the dendritic surface (Fig. 3b, c). In some cases spines appeared to be present even on the neuronal soma itself (Fig. 3b). Indeed, the total number of

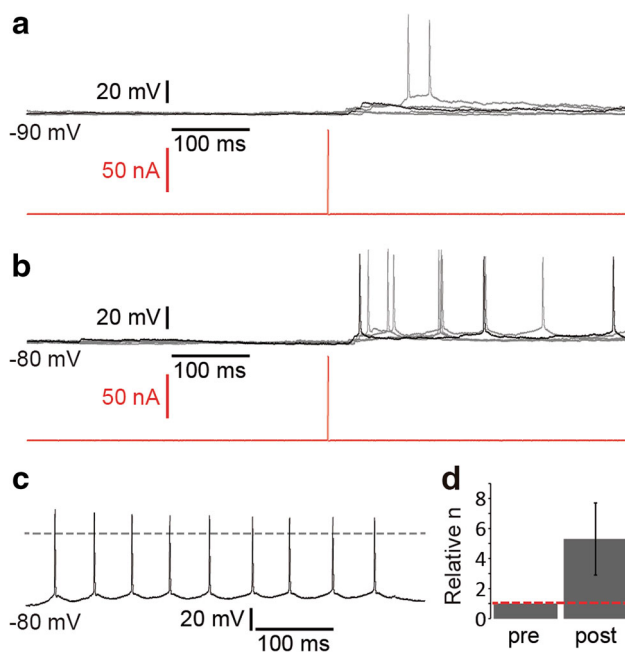


Fig. 2 Functional efficacy of polysynaptic connections. **a** Voltage responses (five consecutive traces, one is highlighted in *black*) of a lateral lamina I LCN kept at -90 mV to stimulation (shown on *bottom*; in *red*) of the presynaptic neuron. **b** The same neuron at a more depolarized membrane potential (around -80 mV) showed increased spike discharge in the post-stimulus period. **c** Spike discharge pattern of the same neuron evoked by a 40 pA depolarizing current injection. *Dashed line* indicates the 0 mV level. **d** Normalized pre- and poststimulus spike numbers for all five neurons showing polysynaptic response to single presynaptic neuron stimulation

spines and spine density both proved to be significantly higher in neurons outside lamina I (OUT/LSN, Fig. 3f, g; $p < 0.01$ and $p < 0.05$, respectively, Student's t test).

Distinct axon trajectories of neurons outside lamina I and in the LSN

Regardless of the location of their somata, the recovered neurons could be grouped into distinct categories on the basis of the type and course of their axons (Table 1). 16 out of 32 successfully recovered neurons (cells 1–7, 10–14, 18, 23, 29 and 31) could be classified based on the presence or absence of a single projecting axon as projection or local-circuit neurons (detailed criteria described in our previous works: Szucs et al. 2010, 2013). Regular PNs gave rise to a single projection axon that originated from the cell body or one of the primary dendrites, crossed the midline in the anterior commissure and ascended in the contralateral anterolateral column (c-ALT). Some of these neurons had collaterals that fell into groups that were previously described in lamina I (Szucs et al. 2010). In 7 cases (cells 9, 15, 21–22, 24, 28 and 30; blue cells in Table 1) the main axon crossed the midline in the posterior commissure and

shortly after entered the medial side of the contralateral anterior column where it started ascending. Another set of neurons (cells 8, 19–20, 27 and 32; $n = 5$, red cells in Table 1) had axons with a similar initial course, but instead of ascending on the contralateral side these axons returned to the ipsilateral side by re-crossing in the anterior commissure and exited into the medial part of the ipsilateral anterior funiculus. Finally, the main axon of the remaining four cells (cells 16–17 and 25–26; green in Table 1), before crossing the midline in the anterior commissure and ascending in the c-ALT, gave rise to two long axon branches one of which ascended in either the ipsilateral DLF (i-DLF) or the ipsilateral dorsal funiculus (i-DF), while the other, showing characteristic features of unmyelinated collaterals, descended in the i-DLF. Although the major grouping criterion was the axon trajectory, neurons divided on this basis also showed other common characteristics described below.

Posterior commissural contralaterally projecting neurons

Neurons belonging to this group showed a spherical organization of their dendrites with the cell body located on the most superficial part rather than the center of this spherical structure. Dendrites protruded out from the soma in a multipolar fashion and occupied a large part of the DLF (Fig. 4a). Dendrites branched frequently even in the vicinity of the soma, thus dendritic segment were generally short (Fig. 4b, c). This type of neuron possessed a high number of short spines (Fig. 4d). Fan-in projection revealed that dendrites showed no preferred orientation filling the space around the soma equally (Fig. 4e). The axon of these neurons started off medially from the soma or proximal dendrites, entered the grey matter and aimed medially towards the central canal. The main axon gave collaterals on the ipsilateral side to various laminae, including lamina X around the central canal (Table 1), and crossed the midline in the posterior commissure. The axon on the contralateral side took a short path ventrally before it exited into the medial side of the anterior column white matter (Fig. 4a). Examination of the spontaneous synaptic input to these neurons revealed occasional, long-lasting and large amplitude EPSPs (Fig. 4f) and EPSCs (Fig. 4g). Summation of these spontaneous events showing generally slow kinetics was not observed.

Double crossing ipsilaterally projecting neurons

In the sample of neurons with unique axon trajectories five neurons possessed a main axon that crossed the midline twice (Fig. 5a). Dendritic arborisation of these cells was

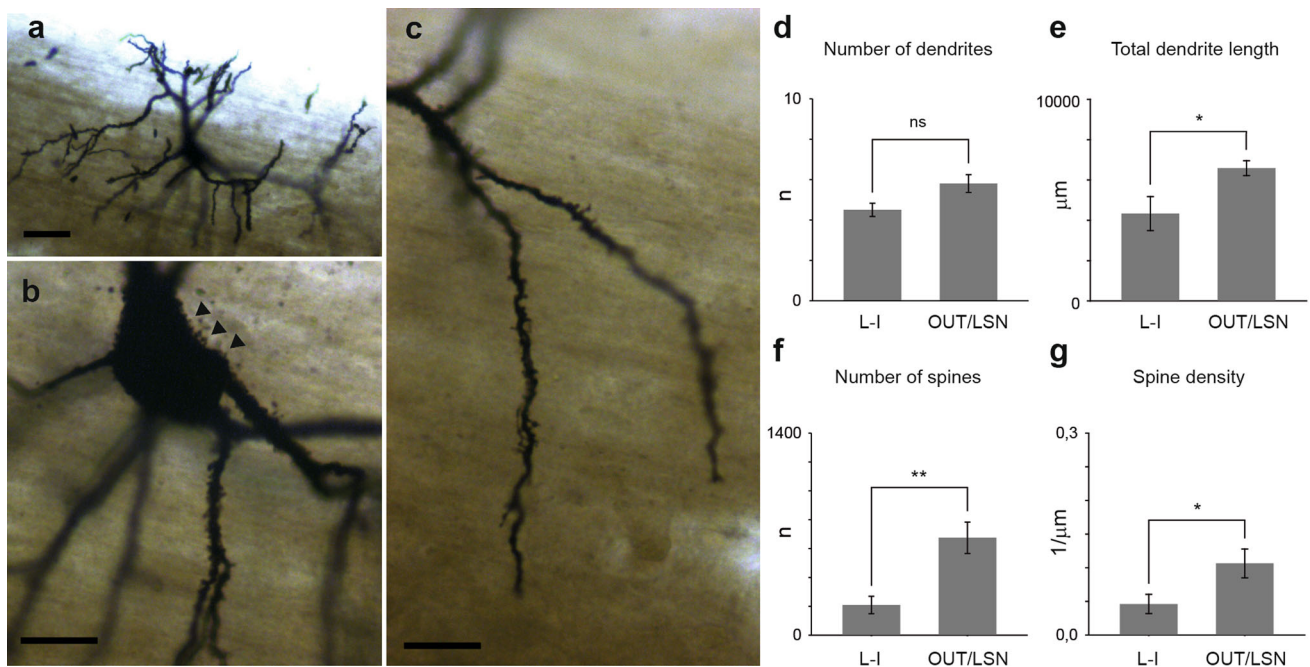


Fig. 3 Somatodendritic characteristics of neurons located laterally to lamina I and in the LSN. **a** Low magnification photograph of a neuron (cell 24 in Table 1) in the LSN, giving rise to numerous not too long, frequently branching dendrites organized in a multipolar fashion. **b**, **c** Dendrites were densely covered with short spines, and spine-like protrusions which were also encountered on certain parts of the soma contour (arrowheads). Scale bars **a** 50 μm; **b**, **c** 20 μm. **d** Mean number of dendrites in our earlier lamina I sample of projection and

local-circuit neurons (L-I; $n = 8$; Luz et al. 2010; Szucs et al. 2013) and cells lateral to the border of the grey matter and in the LSN (OUT/LSN, $n = 15$). **e** Mean total dendrite (reconstructed dendritic segment) length in the same groups of neurons. **f** Mean total number of spines encountered on the dendrites of neurons in the two groups. **g** Mean spine density (total number of spines/total dendrite length) in the two neuron groups. *, $p < 0.05$; Student's t test; **, $p < 0.01$, Student's t test

also dense with numerous branchpoints close to the soma (Fig. 5b, c) and they also presented a high number of spines (Fig. 5d), although less, than neurons crossing in the posterior commissure. However, the orientation of the dendrites were more restricted: they were either going dorsally and followed the curvature of the dorsal grey matter, occupying mostly lamina I–II, or turned ventrally and branched in the DLF. For this reason Fan-in projection showed marked accumulation around 90° (Fig. 5e). The axon started off in the medial direction and aimed towards the posterior commissure giving ipsilateral collaterals in laminae of the deep dorsal horn, intermediate grey matter and around the central canal (lamina X). Interestingly, none of the five neurons gave collaterals to the superficial dorsal horn. The main axon then crossed the midline in the posterior commissure, took a short loop on the contralateral side and re-crossed in the ventral commissure to enter the medial aspect of the white matter in the ipsilateral anterior column (Fig. 5a). Spontaneous synaptic input was more frequent than in the posterior commissure crossing cell group; both EPSPs and EPSCs were showing faster kinetics and occasional summation (Fig. 5f, g).

Bilaterally projecting neurons

Finally, four neurons, two in the LSN and two between the LSN and the edge of the dorsal grey, presented a main axon that, before crossing the line in the anterior commissure, gave rise to an equally strong myelinated-appearing (for criteria see Fig. 5g and text in Szucs et al. 2013) axon branch that entered and ascended in the i-DF or i-DLF. Another characteristic morphological feature was the presence of single thin ipsilateral axon collaterals that had numerous varicosities and descended in the DLF or Lissauer's tract (Table 1). A typical neuron of this type is shown in Fig. 6a. The dendritic tree is quite asymmetric, having most branches filling a conical space in the DLF and having a single branch that spread medially (Fig. 6a). Dendrites were more extensive and branched less frequently than in case of the previous two groups, resulting in longer and less dendritic segments (Fig. 6b, c). Spines were less numerous, not exceeding the values observed earlier in case of neurons in lamina I (L-I, Fig. 3). Fan-in projection confirmed the conic arrangement of dendrites in DLF, showing a prominent accumulation of dendrites at 90°

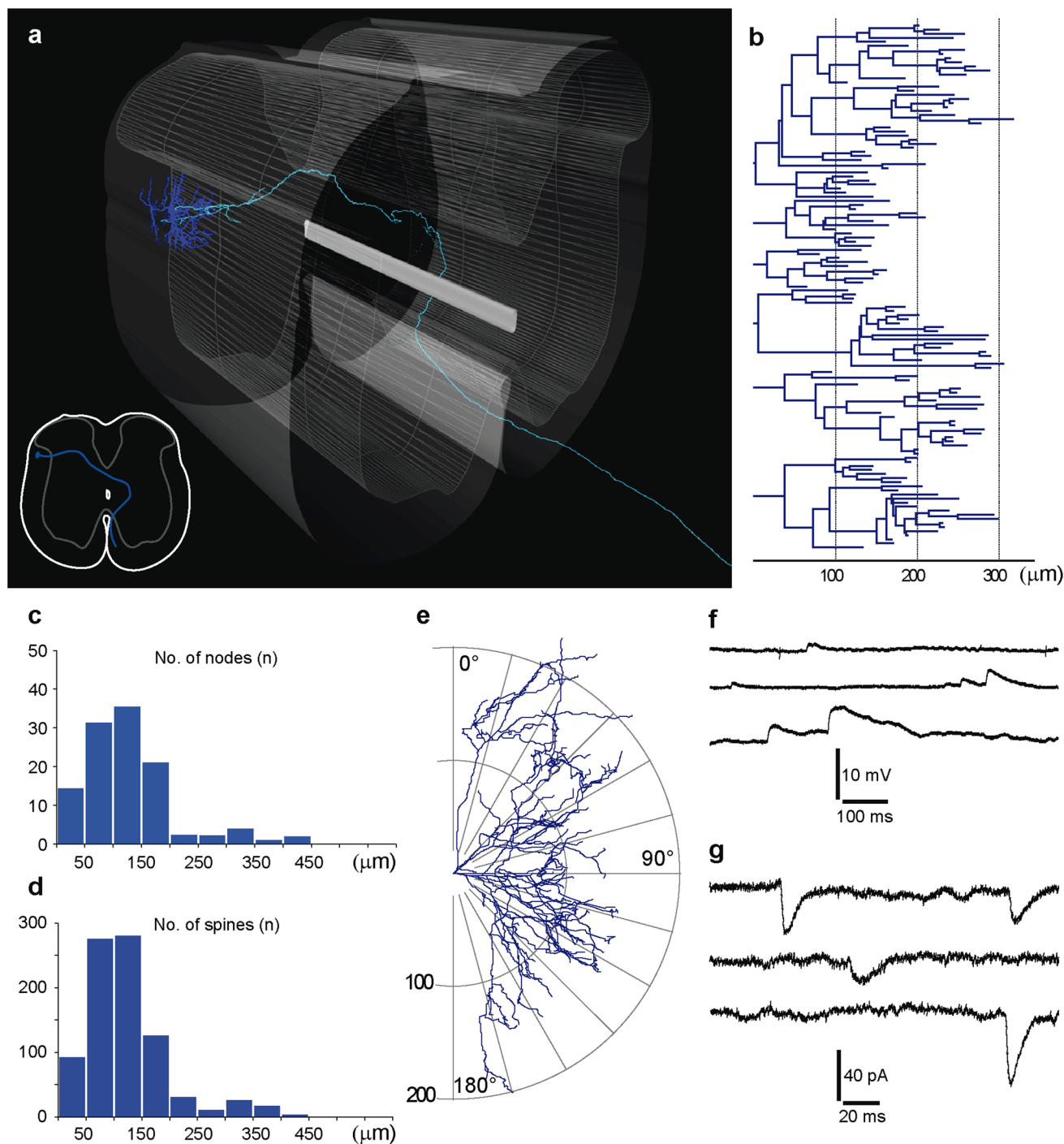


Fig. 4 Morphological description of neurons with their projection axon crossing in the posterior commissure. **a** Three dimensional reconstruction of the neuron (cell 24 in Table 1, also shown on the photographs in Fig. 3) positioned in a schematic spinal cord block. *Inset* shows trajectory of the axon in the transverse plane, crossing the midline in the posterior commissure and exiting into the white matter on the medial side of the anterior column. **b** Dendrogram of the same neuron showing a compact dendritic tree with dense branching in the vicinity of the soma. **c** Sholl analysis of the distribution of nodes

(branch points) and spines (**d**) of the neuron shown in *panel a*. **e** Fan-in diagram (for detailed explanation see “Materials and methods”) of the same neuron. Dendritic processes cover the whole angle-range, showing no preferred orientation. **f** Spontaneous EPSPs recorded at zero injected current in current-clamp mode from three different neurons within this group. **g** Voltage-clamp recordings from the same neurons. The *blue color* used in the figure refers to the color-code of this cell-group in Table 1

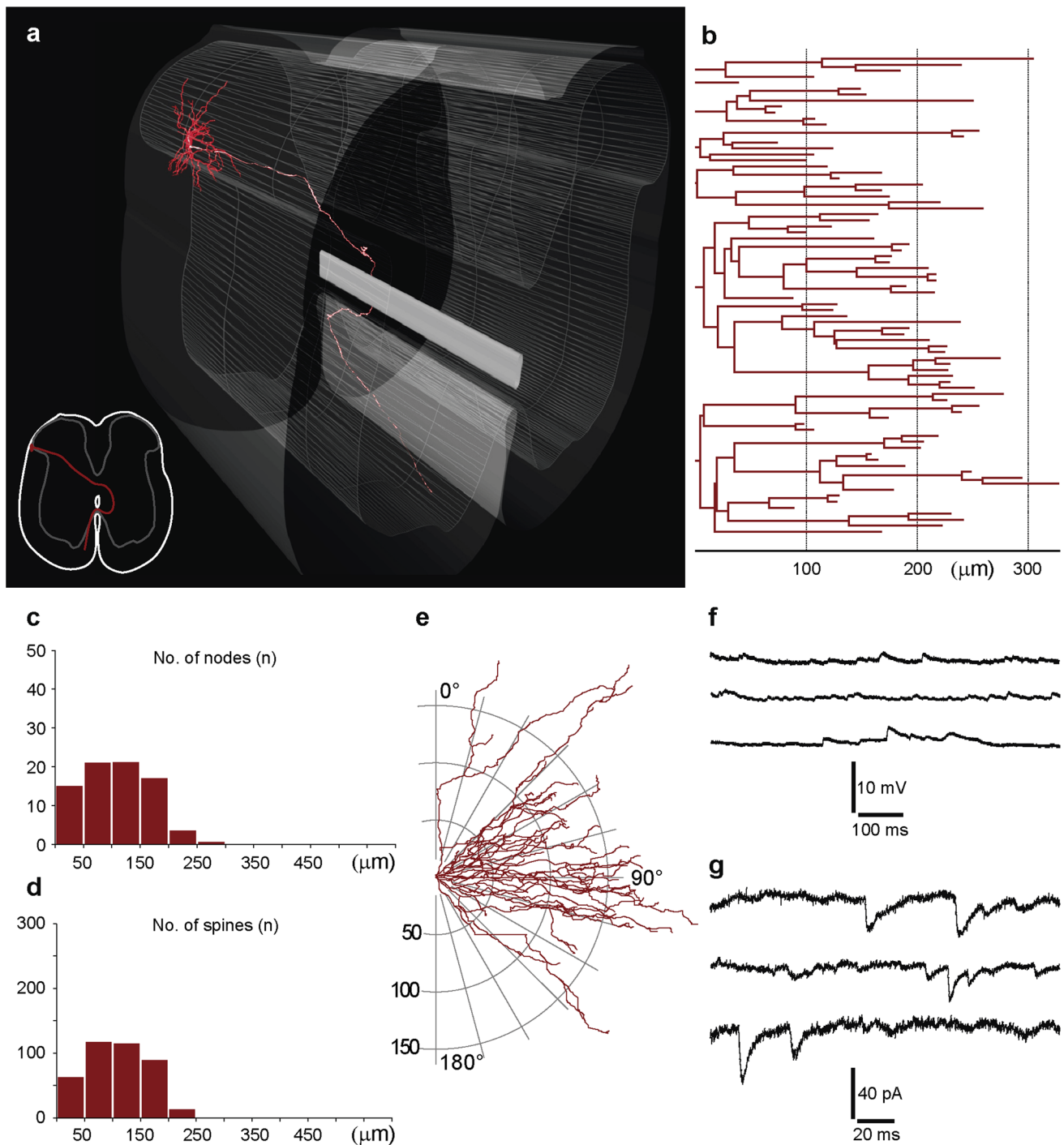


Fig. 5 Morphological features of neurons with double midline crossing ipsilateral projection axon. **a** Three-dimensional reconstruction of a neuron (cell 27 in Table 1) located just outside lamina I, at the lateral edge of the dorsal grey matter. *Inset* shows trajectory of the axon in the transverse plane. The single projection axon of the cell crosses the midline first in the posterior commissure and crosses again in the anterior commissure. The axon then enters the white matter in the medial aspect of the anterior column. **b** Dendrogram of the same neuron showing a relatively compact dendritic tree with less

branching than in case of the neuron in Fig. 4c). Sholl analysis of the distribution of nodes (branch points) and spines (**d**) of the same neuron. **e** Fan-in diagram of the same neuron. Dendritic processes show some preference for the vertical (dorso-ventral) direction, which is apparent from the slight accumulation of processes around 90°. **f** Spontaneous EPSPs recorded at zero injected current in current-clamp mode from three different neurons within this group. **g** Voltage-clamp recordings from the same neurons. The red color used in the figure corresponds to the color code of this cell-group in Table 1

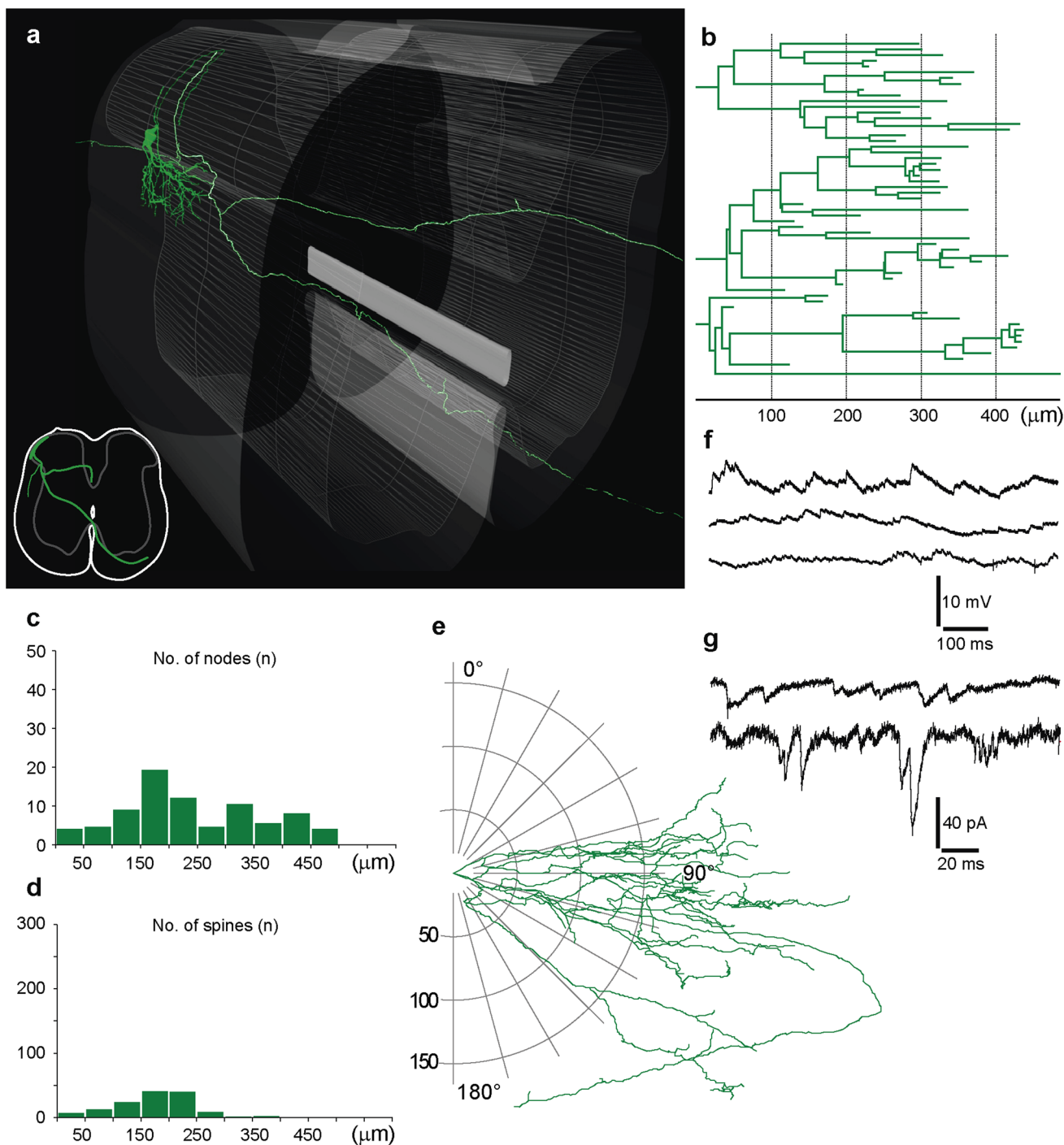


Fig. 6 Morphological description of neurons with bilateral projection axon. **a** Three dimensional reconstruction of a typical, very asymmetric neuron (cell 26 in Table 1) in this group. *Inset* shows trajectory of the axon that, in this case, originates from the single long dendrite that follows the curvature of the dorsal horn. The main axon then splits into two and enters the ipsilateral DF and contralateral anterior column. **b** Dendrogram of the same neuron showing long, slender sparsely branching dendrites. **c** Sholl analysis of the

distribution of nodes (branch points) and spines (**d**) of the neuron shown in *panel a*. **e** Fan-in diagram shows a major preference of dendrites to the vertical direction, with most dendrites reaching ventrally into the DLF. **f** Numerous fast spontaneous EPSPs recorded at the resting potential from three different neurons within this group. **g** Voltage-clamp recordings from the same neurons. The *green color* used in the figure corresponds to the color code of this cell-group in Table 1

(Fig. 6e). Interestingly, despite the fact that these cells had few spines, the frequency of spontaneous excitatory activity was high and all cells in this group showed large number of various amplitude EPSPs and EPSCs that were often superimposed (Fig. 6f, g).

Differences in spontaneous EPSC and EPSP frequency and kinetics

In order to quantitatively analyze the differences in the frequency of spontaneous postsynaptic events (sEPSCs and sEPSPs) we selected, from each neuron, ten traces (length: 200–800 ms) where the presynaptic neuron was not stimulated, calculated the sEPSC frequency for each trace and presented pooled data for the corresponding groups in Fig. 7 ($n = 70$, blue; $n = 40$, green; $n = 40$, red). Statistical analysis proved that bilaterally projecting neurons presented a significantly higher ($p < 0.05$, Kruskal–Wallis one way analysis of variance on ranks followed by Dunn’s pairwise multiple comparison) mean frequency (23.4 ± 2.1 Hz) of spontaneous events than neurons with the other two types of axonal trajectories (6.6 ± 1.1 Hz, blue; 6.4 ± 1.3 Hz, red; Fig. 7a). For measurements of sEPSP and sEPSC kinetic descriptors we selected 7–30 events of each type for each neuron in a

given group (sEPSPs: $n = 67$, blue; $n = 40$, green; $n = 40$, red; sEPSCs: $n = 163$, blue; $n = 60$, green; $n = 90$, red). Spontaneous EPSCs were taken from traces where the presynaptic neuron was not stimulated, while sEPSPs were analyzed using current-clamp traces of the firing pattern protocol (at 0 current step) acquired for each cell. The mean amplitude of sEPSCs was significantly smaller ($p < 0.05$, Kruskal–Wallis one-way analysis of variance on ranks followed by Dunn’s pairwise multiple comparison) in neurons with double crossing ipsilaterally projecting axon (17.6 ± 0.9 pA, red cells; 30.4 ± 1.7 pA, blue neurons; 32.1 ± 3.5 pA, green cells; Fig. 7b, f). The mean sEPSP amplitudes, however, did not show significant differences (1.3 ± 0.1 mV, blue; 1.1 ± 0.1 mV, red; 1.3 ± 0.2 mV, green; Fig. 7c). Mean rise time (measured as time-to-peak) was significantly shorter ($p < 0.05$, Kruskal–Wallis one way analysis of variance on ranks followed by Dunn’s pairwise multiple comparison) in bilaterally projecting neurons for both sEPSCs (2.0 ± 0.1 ms, green; 3.1 ± 0.1 ms, blue; 3.3 ± 0.1 ms, red; Fig. 7d) and sEPSPs (4.1 ± 0.4 ms, green; 8.8 ± 0.4 ms, blue; 7.1 ± 0.4 ms, red; Fig. 7e). The obvious difference in the sEPSC kinetics of averaged traces (Fig. 7f) could be best demonstrated after scaling to the same amplitude (Fig. 7g).

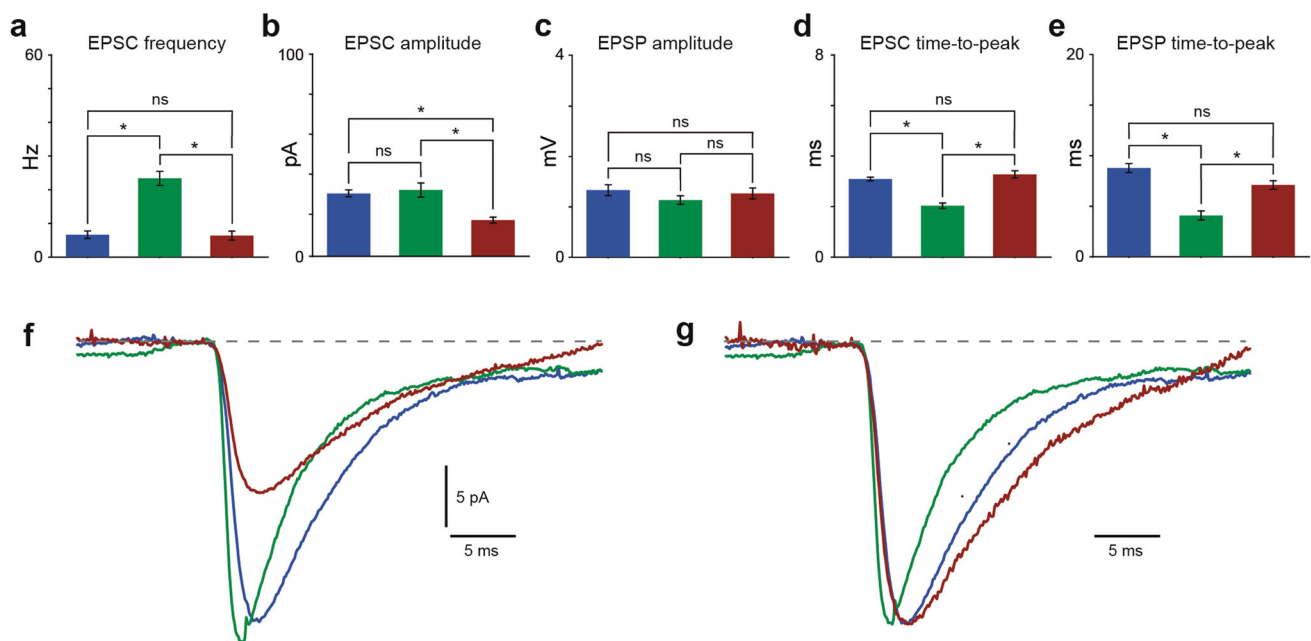


Fig. 7 Comparison of sEPSCs and sEPSPs in the three axon trajectory groups. Colors of the traces and bars used in the graphs correspond to the color codes of the cell-groups in Table 1. **a** Mean sEPSC frequency was significantly higher in neurons with bilateral axon (green). **b** Neurons with double midline crossing ipsilateral projecting axons showed sEPSCs with significantly lower mean amplitude (see also **f**). **c** There was no difference in the mean amplitude of sEPSPs between neurons in the three groups. **d, e** Mean

rise time (measured as time-to-peak) of sEPSCs and sEPSPs was significantly shorter in neurons with bilateral axon (green). **f** The difference in EPSC kinetics is shown on averaged baseline-adjusted and aligned traces **g**) and became more obvious when averaged traces of the three groups were scaled to the same amplitude. Colors of the traces and bars used in the graphs correspond to the color codes of the cell-groups in Table 1. * $p < 0.05$; Kruskal–Wallis one-way analysis of variance on ranks with Dunn’s pairwise multiple comparison

Discussion

In this paper we have tested the hypothesis that rostrally oriented axons in the DLF, comprising, in part, the collaterals of PNs as well as local axon of LCNs, are providing synaptic input to dendrites of lateral lamina I neurons and to neurons located in the LSN. By stimulating superficial cells in the lateral aspect of lamina I we could indeed detect mono- and polysynaptic excitation of LSN and lateral lamina I neurons; these connections, however, were rare. On the other hand, by careful 3-D reconstruction of the neurons, we discovered previously undescribed axon trajectories of putative projection or propriospinal neurons in the lateral dorsal spinal cord.

Technical considerations

Unlike most paired recordings from visually identified neurons where the connected neurons are usually located in the same visual field, we aimed to investigate monosynaptic connections between cells that were remotely located. Even though we used cell-attached stimulation of putative presynaptic neurons, advancing the visual field while keeping the selected postsynaptic neuron in proper whole-cell configuration was very challenging. We continuously monitored the condition of the postsynaptic neuron, but one cannot exclude the possibility that some connections may have been overlooked when evoked event amplitudes fell below detection level due to the progressive deterioration of the seal. Thus, ratios reported here for mono- and polysynaptic propriospinal connections may be underestimations.

The technically challenging recording configuration also required experimentation with young adult animals that are regularly used in electrophysiological studies *in vitro*. While the possibility that short propriospinal connectivity rate may be different in older animals cannot be excluded, it is unlikely that anatomical features such as collaterals embedded in the dense fiber bundles of the DLF would change significantly. Midline crossing of the main axon that is only limited to a short time window during development is even less likely to be altered during further maturation of the animal.

The morphological recovery rate in this study (37 %) was somewhat lower than in our previous works with the same preparation and conditions (Szucs et al. 2010, 2013) and might be due to the increased difficulty of maintaining proper seal conditions among the fibers of the DLF. Nevertheless, this is still higher than the success rate of recovering biocytin filled cells in our previous work on LSN neurons (30 %, Pinto et al. 2010). Probably due to the same reason, we could not achieve presynaptic labeling to an

extent that would have allowed identification of synaptic connections in the initial trials, thus, later we excluded biocytin from the cell-attached pipette to reduce contamination of the preparation that would have made it difficult to trace the axon trajectories.

Short intersegmental connections of lamina I and the LSN are rare but some may be very potent

We demonstrated that neurons outside the dorsal grey matter and in the LSN receive monosynaptic connections from lateral lamina I neurons. Connected neurons were rare and could not be detected at distances above 720 μm in the caudal direction. Such connections may be considered as intersegmental, since upper lumbar segments in animals of the experimental age we used have similar lengths (Szucs et al. 2013). In terms of functionality, these ultra-short propriospinal connections are of questionable importance, but may increase the complexity of intraspinal divergence and convergence (Pinto et al. 2010) of primary afferent inputs. Synaptic delay in the recorded monosynaptic connections showed a large variation, but even the longest observed latencies would be compatible with putative long axodendritic pathways and recording conditions at room temperature (Luz et al. 2010).

A striking observation in this study was the presence of powerful polysynaptic excitation of some neurons in the DLF region. The stimulation of a single presynaptic lamina I neuron evoked long-lasting and suprathreshold excitation of postsynaptic cells. A putative circuitry behind such phenomenon would include a set of excitatory interneurons that spread and amplify the activity of a single “initiator” neuron via feed-forward excitation. The sustained EPSC frequency increase may also be explained by a powerful inhibition of inhibitory interneurons, thus, via disinhibition, the normally silent but now liberated excitatory neurons could be responsible for the frequency increase of EPSCs in target neurons. These mechanisms would require a long-lasting inhibition upon a single transient—although suprathreshold—stimulation of the presynaptic “initiator” neuron. These “initiator” neurons may also be involved in pathological amplification of incoming signals during certain chronic pain conditions, thus identification of them would be crucial. A good candidate for the “conductor” neuron would be those excitatory and inhibitory LCNs in lamina I that have extensive axons that bridge several segments rostrocaudally and have thousands of varicosities, making them capable of providing high excitatory or inhibitory transmitter levels in a large volume of the spinal dorsal horn. Elucidating this question was beyond the scope of this study, but we are presently performing an electron microscopic level analysis of the targets of individually labeled LCN axon terminals.

Neurons in the lateral aspect of the dorsal horn show morphological evidence for integration

With the exception of five cells the majority of neurons in the recovered sample fell outside the dorsal grey matter, some clearly within the boundaries of the longitudinal cell column of the LSN, while others between the edge of the dorsal grey and the LSN. In general organization of the dendrites was very different from PNs and LCNs of lamina I. Neurons close to the dorsal grey were asymmetric having most dendrites protruding into the DLF ventrolaterally, and only a few aimed to the medial direction, running close to the surface within lamina I (see neuron in Fig. 6a). Earlier morphological studies in the LSN described neurons with dendrite oriented either laterally (Bresnahan et al. 1984; Rethelyi 2003), medially (Menetrey et al. 1982; Rethelyi 2003) or rostrocaudally (Rethelyi 2003). LSN neurons in our sample showed a combination of these features and were either spherical (e.g., the neuron in Fig. 4a) or had two main groups of dendrites going ventrolaterally and dorsally (e.g., the neuron in Fig. 5a), filling the DLF almost completely. This difference may be due to the incomplete or random labeling of neuronal processes with the methods used in the previous studies (e.g., Golgi-Kopsch method). Above the dense arborization of dendrites in the DLF, these lateral neurons also possessed a high number of dendritic spines, further increasing the putative contact surface. This efficient coverage of the DLF cross section is in line with the suggestion of Olave and Maxwell 2004 that the LSN may function as an integrative nucleus, where neurons can receive inputs from primary afferents of visceral origin, interneurons and descending pathways from supraspinal loci.

Axon architecture of neurons outside the superficial dorsal grey matter

It has long been known that neurons of the LSN can be retrogradely labeled from various supraspinal loci, including the parabrachial nucleus (Ding et al. 1995; Feil and Herbert 1995), the periaqueductal grey (Pechura and Liu 1986; Harmann et al. 1988) the nucleus of the solitary tract (Menetrey and Basbaum 1987; Esteves et al. 1993), the medullary reticular formation (Leah et al. 1988; Pechura and Liu 1986), the nucleus accumbens, the septum (Burstein and Giesler 1989) and the amygdala and orbital cortex (Burstein and Potrebic 1993). LSN neurons project bilaterally to the mediodorsal thalamic nucleus and some authors assume that this LSN-mediodorsal pathway may be involved in the emotional and cognitive aspects of pain (Gauriau and Bernard 2004). The above morphological evidence implies that the majority of LSN neurons are projection neurons, and this view is also supported by

Rethelyi (2003), who observed that the axons of LSN neurons become myelinated soon after their origin; a common feature of projection axons (Rethelyi 2003). Besides supraspinal targets, LSN neurons also project to lamina I, II, V and VII of the spinal cord (Jansen and Loewy 1997).

In good agreement with the above, in this study we found that most neurons outside the dorsal grey matter (24 out of 27)—including LSN neurons—had a myelinated-appearing projecting axon and 20 had ipsilateral collaterals within almost all laminae of the spinal grey matter. Despite the above one cannot rule out the possibility that some of these cells could be propriospinal neurons, since axons running in the anterolateral funiculus were shown to form inter-enlargement pathways between the cervical and lumbar spinal cord (Reed et al. 2006). Furthermore, contralateral lumbosacral lamina I neurons have been retrogradely labeled after tracer injections into the cervical ventral horn and some of them look very similar to bilaterally projecting cells of our study (Fig. 1i in Dutton et al. 2006). Such labeling, however, could have resulted from uptake of tracer by projection neuron axons of passage, located in the same anterolateral funiculus (Dutton et al. 2006). Thus, further experiments with prior retrograde labeling of projection neurons from supraspinal centers will be needed to clarify the exact function of the neurons described in our study.

Similarly to our earlier observations (Szucs et al. 2010, 2013) dendritic origin of the axon was also frequent among neurons outside lamina I and in the LSN. The most remote axon initiation ($\sim 90 \mu\text{m}$) occurred in one of the bilateral projection neurons, shown in Fig. 6a, where the axon originated from the single medially oriented loopy dendrite. This observation enforces earlier results of computer simulations (Lee et al. 2005) and suggestions (Szucs et al. 2010) that both the distal and proximal part of the dendrite giving rise to an axon may have very important roles in the regulation of action potential initiation. Indeed, with the help of modern techniques, in a recent study authors provided functional evidence for the influence of dendritic axon origin on action potential initiation (Thome et al. 2014).

Projecting axon of neurons located outside the dorsal grey matter may also cross the midline in the posterior commissure

The mechanisms that govern axon midline crossing during development have been well studied, particularly at the spinal cord (Escalante et al. 2013). Attracting and repellent factors such as Netrin1, Sonic-Hedgehog, secreted by the floor-plate and roof-plate were shown to act in a complementary and sequential manner to guide sets of axons

within the developing CNS (Augsburger et al. 1999). While lamina I projection neurons in our works (Szucs et al. 2010), without exception, crossed the midline in the anterior commissure, neurons outside the dorsal grey matter and in the LSN showed other axon trajectories. In seven cases the main axon crossed the midline in the posterior commissure and continued to ascend in the medial part of the anterior column white matter. These axons may be among those reported by Petko and Antal 2000 crossing the midline in the posterior commissure after BDA injection into the lateral part of lamina III and IV, where the anterograde tracer may have been picked up also by neurons located in the DLF. Midline crossing in the posterior instead of the anterior commissure may be the result of different responsiveness of the path-finding axon cone or a temporal difference in neuronal development that results in missing the time-window for regular crossing in the anterior commissure. Anterograde tracing of posterior commissure crossing axons will be important to define targets and function of these neurons.

Axon trajectory of double crossing ipsilaterally projecting neurons oppose our present knowledge on axon midline guidance

The finding that five neurons in our sample possessed axons that ascended in the ipsilateral white matter is not striking in itself, since lamina I neurons, most of them belonging to the multipolar somatodendritic type, have been reported to be projecting ipsilaterally to the dorsal reticular nucleus (Lima 1998). On the other hand, the fact that the projection axon in these five cases crosses the midline twice is not compatible with our present knowledge on axon midline guidance. Prior to midline crossing, commissural axons are attracted by floor plate-derived Netrin-1 and Sonic Hedgehog (Kennedy et al. 1994; Charron et al. 2003). After crossing, repellents of the Slit and Semaphorin families expel axons from the floor plate and prevent re-crossing (Zou et al. 2000; Long et al. 2004). Slits act through receptors of the Robo family. Robo3, which is expressed exclusively in commissural neurons, produces two splice isoforms with opposite activities (Sabatier et al. 2004; Chen et al. 2008). Robo 3.1 is expressed on pre-crossing axons and suppresses premature responsiveness to Slits, thereby allowing midline crossing; Robo 3.2 localizes to post-crossing axons and acts as a classical Slit receptor that contributes to midline repulsion (Chen et al. 2008), thus rendering re-crossing impossible. In this paper, however, we show, for the first time, that there are ipsilaterally projecting neurons that cross the midline twice: first in the posterior commissure and then, after taking a short path in the contralateral grey, for a second time in the anterior commissure. Although the molecular

program that determines axonal ipsilaterality in the spinal cord is poorly understood, recently, ipsilateral neurons whose axons grow in close proximity to the midline, such as the ascending dorsospinal tracts and the rostromedial thalamocortical projection, were demonstrated to avoid midline crossing because they transiently activate the transcription factor *Zic2*. In contrast, uncrossed neurons whose axons never approach the midline control axonal laterality by *Zic2*-independent mechanisms (Escalante et al. 2013). This explanation, however, implies that ipsilateral axons stay on the same side without crossing the midline. Our observation suggests that there are other, yet unresolved molecular mechanisms that govern axon crossing through the midline. Further tracing and lineage analysis studies will be necessary to elucidate the function and origin of these neurons.

Bilaterally projecting axons

Apart from the neurons with posterior commissure crossing and double crossing projecting axons, four cells in our sample had bifurcating myelinated-appearing axons. The main axon in these cells bifurcated within the dorsal grey matter and while one branch followed the regular path of PNs, the other one entered the dorsal funiculus and ascended there in the ipsilateral side. Lamina I PNs with collaterals crossing the midline at the supraspinal level and thus achieving bilateral projections have been reported before (Al-Khater and Todd 2009). In case of the four bilateral projection neurons in our sample the splitting of the main axon occurs earlier and the two equally strong branches seemingly ascend in different tracts from the beginning. Since LSN is known to project bilaterally to the mediodorsal thalamic nucleus (Gauriau and Bernard 2004), it would be tempting to say that bilaterally projecting neurons may contribute to this double projection. However, from a metabolic point of view, bilateral projection this way would be very inefficient due to the high energy cost of maintaining the two branches. It is more likely that the ipsilateral branch is establishing long propriospinal connections on the ipsilateral side while the contralateral branch ascends to supraspinal targets. Indeed, LSN neurons could be double labeled from two injection sites in the brain stem and diencephalon, as well as in the brainstem and spinal cord (Rethelyi 2003), which raised the possibility that these neurons probably take part in the establishment of propriospinal connections via collateral axon branches. Furthermore, when the retrograde tracer cholera toxin beta-subunit (CTB) was used to trace long ascending propriospinal projections from neurons in the lumbosacral spinal cord to the upper cervical gray matter some lumbosacral superficial dorsal horn neurons were identified. These propriospinal projections were suggested to be

involved in coordinating head and neck movements during locomotion or stimulus-evoked motor responses (Dutton et al. 2006). In addition, LSN neurons in the upper cervical segments can be labeled from the upper thoracic segments (Verburgh et al. 1990). Conversely, anterogradely labeled axons of the LSN neurons located in cervical segments have been detected around the neurons in the intermediolateral nucleus in the middle thoracic segments (Jansen and Loewy 1997). This caudal propriospinal connection is supported by our finding that bilateral neurons in the LSN and outside the dorsal grey also issued long but thin caudal collaterals in the ipsilateral DLF or Lissauer-tract.

Conclusions

Our findings indicate that propriospinal connections from lamina I PNs and LCNs onto other lamina I and LSN neurons are not frequent but some are extremely potent. The later may be important in sustained nociceptive signalling during pathological conditions. We revealed unique axon trajectories of putative projection or propriospinal neurons in the lateral aspect of the dorsal horn and in the LSN that suggest a development different from the regular lamina I projection cells. While LSN is not present in all species the novel axon trajectories revealed in our study may help to identify cell groups with analogous function and developmental origin in other species. Our findings emphasize the importance of understanding the connectivity matrix of the superficial dorsal horn in order to decipher spinal sensory information processing.

Acknowledgments This work was supported by FEDER funds through the Operational Competitiveness Programme—COMPETE and by national funds through FCT—Fundação para a Ciência e a Tecnologia under the project FCOMP-01-0124-FEDER-029632 (PTDC/NEU-SCC/0347/2012 to BS), the Hungarian Academy of Sciences (MTA-TKI 242 to MA), the János Bolyai Research Scholarship of the Hungarian Academy of Sciences (PSz), the Hungarian Brain Research Program (KTIA_NAP_13-2-2014-0005 to PSz and KTIA_NAP_13-1-2013-0001 to MA) and TÁMOP-4.2.4.A/2-11/1-2012-0001 ‘National Excellence Program’ supported by the State of Hungary and the European Union, co-financed by the European Social Fund (ZsA). The authors are grateful to Raquel Pinho for her excellent help with the histological processing and reconstruction.

References

- Aguiar P, Sousa M, Szucs P (2013) Versatile morphometric analysis and visualization of the three-dimensional structure of neurons. *Neuroinformatics* 11(4):393–403
- Al-Khater KM, Todd AJ (2009) Collateral projections of neurons in laminae I, III, and IV of rat spinal cord to thalamus, periaqueductal gray matter, and lateral parabrachial area. *J Comp Neurol* 515(6):629–646
- Augsburger A, Schuchardt A, Hoskins S, Dodd J, Butler S (1999) BMPs as mediators of roof plate repulsion of commissural neurons. *Neuron* 24(1):127–141
- Braz J, Solorzano C, Wang X, Basbaum AI (2014) Transmitting pain and itch messages: a contemporary view of the spinal cord circuits that generate gate control. *Neuron* 82(3):522–536
- Bresnahan JC, Ho RH, Beattie MS (1984) A comparison of the ultrastructure of substance P and enkephalin-immunoreactive elements in the nucleus of the dorsal lateral funiculus and laminae I and II of the rat spinal cord. *J Comp Neurol* 229(4):497–511
- Burstein R, Giesler GJ Jr (1989) Retrograde labeling of neurons in spinal cord that project directly to nucleus accumbens or the septal nuclei in the rat. *Brain Res* 497(1):149–154
- Burstein R, Potrebic S (1993) Retrograde labeling of neurons in the spinal cord that project directly to the amygdala or the orbital cortex in the rat. *J Comp Neurol* 335(4):469–485
- Burstein R, Cliffer KD, Giesler GJ Jr (1990) Cells of origin of the spinohypothalamic tract in the rat. *J Comp Neurol* 291(3):329–344
- Charron F, Stein E, Jeong J, McMahon AP, Tessier-Lavigne M (2003) The morphogen sonic hedgehog is an axonal chemoattractant that collaborates with netrin-1 in midline axon guidance. *Cell* 113(1):11–23
- Chen Z, Gore BB, Long H, Ma L, Tessier-Lavigne M (2008) Alternative splicing of the Robo3 axon guidance receptor governs the midline switch from attraction to repulsion. *Neuron* 58(3):325–332
- Cliffer KD, Urca G, Elde RP, Giesler GJ Jr (1988) Studies of peptidergic input to the lateral spinal nucleus. *Brain Res* 460(2):356–360
- Ding YQ, Takada M, Shigemoto R, Mizumo N (1995) Spinoparabrachial tract neurons showing substance P receptor-like immunoreactivity in the lumbar spinal cord of the rat. *Brain Res* 674(2):336–340
- Dutton RC, Carstens MI, Antognini JF, Carstens E (2006) Long ascending propriospinal projections from lumbosacral to upper cervical spinal cord in the rat. *Brain Res* 1119(1):76–85
- Escalante A, Murillo B, Morenilla-Palao C, Klar A, Herrera E (2013) Zic2-dependent axon midline avoidance controls the formation of major ipsilateral tracts in the CNS. *Neuron* 80(6):1392–1406
- Esteves F, Lima D, Coimbra A (1993) Structural types of spinal cord marginal (lamina I) neurons projecting to the nucleus of the tractus solitarius in the rat. *Somatosen Mot Res* 10(2):203–216
- Etlin A, Blivis D, Ben-Zwi M, Lev-Tov A (2010) Long and short multifunicular projections of sacral neurons are activated by sensory input to produce locomotor activity in the absence of supraspinal control. *J Neurosci* 30(31):10324–10336
- Feil K, Herbert H (1995) Topographic organization of spinal and trigeminal somatosensory pathways to the rat parabrachial and Kolliker-Fuse nuclei. *J Comp Neurol* 353(4):506–528
- Gauriau C, Bernard JF (2004) A comparative reappraisal of projections from the superficial laminae of the dorsal horn in the rat: the forebrain. *J Comp Neurol* 468(1):24–56
- Giesler GJ Jr, Elde RP (1985) Immunocytochemical studies of the peptidergic content of fibers and terminals within the lateral spinal and lateral cervical nuclei. *J Neurosci* 5(7):1833–1841
- Gwyn DG, Waldron HA (1968) A nucleus in the dorsolateral funiculus of the spinal cord of the rat. *Brain Res* 10(3):342–351
- Gwyn DG, Waldron HA (1969) Observations on the morphology of a nucleus in the dorsolateral funiculus of the spinal cord of the guinea-pig, rabbit, ferret and cat. *J Comp Neurol* 136(2):233–236
- Harmann PA, Carlton SM, Willis WD (1988) Collaterals of spinohypothalamic tract cells to the periaqueductal gray: a fluorescent double-labeling study in the rat. *Brain Res* 441(1–2):87–97

- Jansen AS, Loewy AD (1997) Neurons lying in the white matter of the upper cervical spinal cord project to the intermedialateral cell column. *Neuroscience* 77(3):889–898
- Juvin L, Simmers J, Morin D (2005) Propriospinal circuitry underlying interlimb coordination in mammalian quadrupedal locomotion. *J Neurosci* 25(25):6025–6035
- Kato G, Kawasaki Y, Koga K, Uta D, Kosugi M, Yasaka T, Yoshimura M, Ji RR, Strassman AM (2009) Organization of intralaminar and translaminar neuronal connectivity in the superficial spinal dorsal horn. *J Neurosci* 29(16):5088–5099
- Kennedy TE, Serafini T, de la Torre JR, Tessier-Lavigne M (1994) Netrins are diffusible chemotropic factors for commissural axons in the embryonic spinal cord. *Cell* 78(3):425–435
- Leah J, Menetrey D, de Pommery J (1988) neuropeptides in long ascending spinal tract cells in the rat: evidence for parallel processing of ascending information. *Neuroscience* 24(1):195–207
- Lee DC, Jensen AL, Schiefer MA, Morgan CW, Grill WM (2005) Structural mechanisms to produce differential dendritic gains. *Brain Res* 1033(2):117–127
- Lima D (1998) Anatomical basis for the dynamic processing of nociceptive input. *Eur J Pain* 2(3):195–202
- Lima D, Coimbra A (1986) A Golgi study of the neuronal population of the marginal zone (lamina I) of the rat spinal cord. *J Comp Neurol* 244(1):53–71
- Long H, Sabatier C, Ma L, Plump A, Yuan W, Ornitz DM, Tamada A, Murakami F, Goodman CS, Tessier-Lavigne M (2004) Conserved roles for Slit and Robo proteins in midline commissural axon guidance. *Neuron* 42(2):213–223
- Lu Y, Perl ER (2003) A specific inhibitory pathway between substantia gelatinosa neurons receiving direct C-fiber input. *J Neurosci* 23(25):8752–8758
- Lu Y, Perl ER (2005) Modular organization of excitatory circuits between neurons of the spinal superficial dorsal horn (laminae I and II). *J Neurosci* 25(15):3900–3907
- Luz LL, Szucs P, Pinho R, Safronov BV (2010) Monosynaptic excitatory inputs to spinal lamina I anterolateral-tract-projecting neurons from neighbouring lamina I neurons. *J Physiol* 588(2):4489–4505
- Menetrey D, Basbaum AI (1987) Spinal and trigeminal projections to the nucleus of the solitary tract: a possible substrate for somatovisceral and viscerovisceral reflex activation. *J Comp Neurol* 255(3):439–450
- Menetrey D, Chaouch A, Binder D, Besson JM (1982) The origin of the spinomesencephalic tract in the rat: an anatomical study using the retrograde transport of horseradish peroxidase. *J Comp Neurol* 206(2):193–207
- Olave MJ, Maxwell DJ (2004) Axon terminals possessing alpha2C-adrenergic receptors densely innervate neurons in the rat lateral spinal nucleus which respond to noxious stimulation. *Neuroscience* 126(2):391–403
- Pechura CM, Liu RP (1986) Spinal neurons which project to the periaqueductal gray and the medullary reticular formation via axon collaterals: a double-label fluorescence study in the rat. *Brain Res* 374(2):357–361
- Petko M, Antal M (2000) Propriospinal afferent and efferent connections of the lateral and medial areas of the dorsal horn (laminae I–IV) in the rat lumbar spinal cord. *J Comp Neurol* 422(2):312–325
- Petko M, Veress G, Vereb G, Storm-Mathisen J, Antal M (2004) Commissural propriospinal connections between the lateral aspects of laminae III–IV in the lumbar spinal cord of rats. *J Comp Neurol* 480(4):364–377
- Pinto V, Szucs P, Lima D, Safronov BV (2010) Multisegmental A δ - and C-fiber input to neurons in lamina I and the lateral spinal nucleus. *J Neurosci* 30(6):2384–2395
- Reed WR, Shum-siu A, Onifer SM, Magnuson DSK (2006) Inter-enlargement pathways in the ventrolateral funiculus of the adult rat spinal cord. *Neuroscience* 142:1195–1207
- Rethelyi M (2003) Neurons of the lateral spinal nucleus in the rat spinal cord—a Golgi study. *Eur J Anat* 7(1):8
- Sabatier C, Plump AS, Le M, Brose K, Tamada A, Murakami F, Lee EY, Tessier-Lavigne M (2004) The divergent Robo family protein rig-1/Robo3 is a negative regulator of slit responsiveness required for midline crossing by commissural axons. *Cell* 117(2):157–169
- Safronov BV, Pinto V, Derkach VA (2007) High-resolution single-cell imaging for functional studies in the whole brain and spinal cord and thick tissue blocks using light-emitting diode illumination. *J Neurosci Methods* 164(2):292–298
- Santos SF, Rebelo S, Derkach VA, Safronov BV (2007) Excitatory interneurons dominate sensory processing in the spinal substantia gelatinosa of rat. *J Physiol* 581(Pt 1):241–254
- Santos SF, Luz LL, Szucs P, Lima D, Derkach VA, Safronov BV (2009) Transmission efficacy and plasticity in glutamatergic synapses formed by excitatory interneurons of the substantia gelatinosa in the rat spinal cord. *PLoS One* 4(11):e8047
- Seybold V, Elde R (1980) Immunohistochemical studies of peptidergic neurons in the dorsal horn of the spinal cord. *J Histochem Cytochem* 28(4):367–370
- Sugiura Y, Terui N, Hosoya Y (1989) Difference in distribution of central terminals between visceral and somatic unmyelinated (C) primary afferent fibers. *J Neurophysiol* 62(4):834–840
- Szentagothai J (1964) Neuronal and synaptic arrangement in the substantia gelatinosa Rolandi. *J Comp Neurol* 122:219–239
- Szucs P, Pinto V, Safronov BV (2009) Advanced technique of infrared LED imaging of unstained cells and intracellular structures in isolated spinal cord, brainstem, ganglia and cerebellum. *J Neurosci Methods* 177(2):369–380
- Szucs P, Luz LL, Lima D, Safronov BV (2010) Local axon collaterals of lamina I projection neurons in the spinal cord of young rats. *J Comp Neurol* 518(14):2645–2665
- Szucs P, Luz LL, Pinho R, Aguiar P, Antal Z, Tiong SY, Todd AJ, Safronov BV (2013) Axon diversity of lamina I local-circuit neurons in the lumbar spinal cord. *J Comp Neurol* 521(12):2719–2741
- Thome C, Kelly T, Yanez A, Schultz C, Engelhardt M, Cambridge SB, Both M, Draguhn A, Beck H, Egorov AV (2014) Axon-carrying dendrites convey privileged synaptic input in hippocampal neurons. *Neuron* 83(6):1418–1430
- Todd AJ (2010) Neuronal circuitry for pain processing in the dorsal horn. *Nat Rev Neurosci* 11(12):823–836
- Verburgh CA, Voogd J, Kuypers HG, Stevens HP (1990) Propriospinal neurons with ascending collaterals to the dorsal medulla, the thalamus and the tectum: a retrograde fluorescent double-labeling study of the cervical cord of the rat. *Exp Brain Res* 80(3):577–590
- Zou Y, Stoekli E, Chen H, Tessier-Lavigne M (2000) Squeezing axons out of the gray matter: a role for slit and semaphorin proteins from midline and ventral spinal cord. *Cell* 102(3):363–375